Quantifying the opal belt in the Atlantic and Southeast Pacific Sector of the Southern Ocean by means of ^{230}Th-normalization

Walter Geibert[*1], Michiel M. Rutgers van der Loeff[1], Regina Usbeck[2], Rainer Gersonde[1], Gerhard Kuhn[1], and Jens Seeberg-Elverfeldt[1]

*corresponding author

[1]Alfred Wegener Institute for Polar and Marine Research

Am Handelshafen 12

27570 Bremerhaven,Germany

++49 471 4831 1287 (Phone)

++49 471 4831 1425 (Fax)

*corresponding author: wgeibert@awi-bremerhaven.de

[2]FIELAX Company for Scientific Data Management,

Schifferstrasse 10-14

27568 Bremerhaven,Germany

Abstract

A set of 114 samples from the sediment surface of the Atlantic, Eastern Pacific and Western Indian sectors of the Southern Ocean has been analyzed for ^{230}Th and biogenic silica. Maps of opal content, Th-normalized mass flux, and Th-normalized biogenic opal flux into the sediment have been derived. Significant differences in sedimentation patterns between the regions can be detected. The mean bulk vertical fluxes integrated into the sediment in the open Southern Ocean are found in a narrow range from 2.9 $g*m^{-2}*yr^{-1}$ (Eastern Weddell Gyre) to 15.8 $g*m^{-2}*yr^{-1}$ (Indian Sector), setting upper and lower limits to the vertically received fraction of open ocean sediments. The silica flux to sediments of the Atlantic sector of the Southern Ocean is found to be $4.2 \pm 1.4 * 10^{11}$ $mol*yr^{-1}$, just one half of the last estimate. This adjustment represents 6 % of the output term in the global marine silica budget.

INDEX TERMS:

1050 Geochemistry: Marine geochemistry (4835, 4850)

3022 Marine Geology and Geophysics: Marine sediments-processes and transport

4805 Oceanography: Biological and Chemical: Biogeochemical cycles (1615)

4860 Oceanography: Biological and Chemical: Radioactivity and Radioisotopes

4863 Oceanography: Biological and Chemical: Sedimentation

KEYWORDS: ^{230}Th, opal, silica, focusing

1 Introduction

Since the expedition of the H.M.S. Challenger from 1873 to 1876, it has been recognized that considerable areas of the deep-sea floor surrounding Antarctica are covered by siliceous sediments [*Thomson and Murray,* 1891]. Extensive mapping of marine sediments has later on improved our knowledge about the distribution of such sediments. Probably, the most comprehensive data collection on global opal distribution, composed of more than 2000 individual samples, was presented by *Lisitzin* [1971]. The frequently cited maps of *Lisitzin* [1971, 1985, 1996] displayed three regions of siliceous deposits: the north Pacific, the equatorial Pacific, and, by far the most important, a continuous belt around Antarctica. So far, the circum-antarctic occurrence of siliceous deposits, called the "opal belt", was founded on the measurement of silica concentrations, not on silica fluxes.

After the introduction of suitable dating techniques, sediment accumulation rates could be derived. The classical work of *DeMaster* [1981] reports sedimentation rates of 3.5 to 16.8 $cm*kyr^{-1}$ in the Southern Ocean, 55 % of which were assumed to consist of biogenic silica. A later work of *DeMaster et al.* [1991] gave even higher rates for sediment accumulation in the Atlantic Sector of the Southern Ocean, with 20-180 $cm*kyr^{-1}$. Many more cores with similarly high sedimentation rates have been described since. Extrapolation of the limited number of dated cores to the entire opal belt led to the long-standing estimate that roughly 70% of the world silica inputs are deposited in the opal belt [*DeMaster*, 1981; *Nelson et al.*, 1995; *Tréguer et al.*, 1995].

This concept changed dramatically when the extent of sediment redistribution by bottom currents in the Antarctic Circumpolar Current (ACC), already suspected from studies of ^{210}Pb near Maud Rise [*van Bennekom et al.*, 1988], became apparent from budget studies of ^{230}Th [*François et al.*, 1993]. In fact, *DeMaster* [1979] had already observed that the inventory of

^{230}Th in his high-accumulation cores was an order of magnitude higher than expected from production in the water column. He had explained this by excess scavenging by the supposedly high particle fluxes in the water column. Studies of the distribution of ^{230}Th in the water column showed this explanation to be incorrect [*Rutgers van der Loeff and Berger*, 1993], implying that the high inventories could only be explained by sediment focusing.--. Focusing factors well above unity in the Southern Ocean as reported by *François et al.* [1993] or *Frank et al.* [2000] give evidence of a systematic bias in the available core material towards high sedimentation rates. This is easily explained by the requirements of climate studies for cores with high temporal resolution, which can be met by modern high-resolution seismics and increasingly accurate ship positioning.

During the last 20 years, the understanding of ^{230}Th as a tool for the reconstruction of vertical particle fluxes has constantly been improved, providing us now with a well developed method to correct for lateral sediment redistribution with basically known uncertainties [*François et al.*, 2004]. The revised view of focusing-corrected accumulation rates has already helped to reconcile apparent inconsistencies between production and accumulation rates [*Pondaven et al.*, 2000; *Nelson et al.*, 2002] and has led to a preliminary adjustment of the estimate for total opal accumulation rates in the Southern Ocean [*Ragueneau et al.*, 2000; *DeMaster*, 2002]. In the last years, some Th-normalized silica fluxes from different basins of the Southern Ocean have been made available, mostly on longitudinal sections [*François et al.*, 1997; *Frank et al.*, 1999; *Pondaven et al.*, 2000; *Sayles et al.*, 2001; *Dezileau et al.*, 2003], but a revision of the concept of the opal belt in terms of the spatial distribution of accumulation rates still stands out.

Besides the bias introduced to budget calculations by sediment redistribution, additional uncertainty has been added by a lack of knowledge about the spatial extent of siliceous deposits in the Southern Ocean. The early map of silica contents given by *Lisitzin* [1971] was indicating the circumpolar occurrence of siliceous deposits around Antarctica. In 1977, *Cooke*

and Hays [1982] were presenting a map on sediment types around Antarctica, elucidating the shift in sedimentation processes between glacial and interglacial times. Their dataset had a gap in the Southeast Pacific and the Scotia Sea, preventing further conclusions about sedimentation between 90°W and 30°W. However, this map was underlying some publications that have largely influenced our current understanding of the opal belt. *DeMaster* [1981], *Burckle et al.* [1982], *Broecker and Peng* [1982], and *Tréguer and van Bennekom* [1991] have referred directly or indirectly to the map of Cooke and Hays when showing the distribution of siliceous sediments around Antarctica, with a gap in siliceous deposits in the region where Cooke and Hays had no data. Recent investigations [*Zielinski and Gersonde*, 1997; *Schlüter et al.*, 1998] pointed out that this gap in siliceous sediments is non-existent. This is of particular importance for the calculation of budgets, which require a good knowledge about the spatial extent of the region of highly siliceous deposits. As a result of the poorly constrained boundaries of siliceous deposits, considerably differing estimates of the surface area of the opal belt have been used in budget calculations. For example, *DeMaster* [1981] gives estimates for the annual flux of silica to the South Atlantic Ocean, assuming an area of $1.9*10^{16}$ cm^2 to be covered by siliceous deposits. In 2002, *DeMaster* estimates the extent of this area to be $5.1*10^{16}$ cm^2. *Schlüter et al.* [1998] consider an area of $9.5 * 10^{16}$ cm^2 to represent opal deposition in the South Atlantic, including the sediments of the Scotia Sea, which they show to receive considerable inputs of biogenic silica. Obviously, not only the determination of accumulation rates is crucial for the calculation of the silica budget, but also a common reference describing the spatial extent of siliceous deposits.

Moreover, the selection of appropriate methods for sampling and analysis is essential for the accurate determination of recent fluxes into the sediment. Long cores, taken by gravity or piston corers, may suffer from substantial losses at the core-top. Another problem is the analysis of biogenic silica. Different methods have been shown to yield considerably differing results [*Conley*, 1998; *Schlüter and Rickert*, 1998], and care has to be taken when comparing

results obtained by different methods. In order to present a consistent dataset, we have chosen to ignore some results from earlier studies, although this means we cannot present a circumpolar map of silica deposition yet.

Consequently, we first set out to describe how appropriate sample material has been chosen, and to give details about the methods used. For the ^{230}Th-normalization, we discuss the errors that may be introduced into the data by violating model assumptions. Then we present new maps of opal contents, total sediment rain rates, and focusing-corrected opal fluxes into the sediments of the Atlantic, SE Pacific, and Western Indian sectors of the Southern Ocean. Based on these maps, we select regions of similar sedimentation, and describe how the regions have been defined. These definitions are used to calculate budgets of fluxes into the sediments of the Southern Ocean. We compare our results to earlier estimates, and discuss why the differences are so large.

2 Methods

2.1 Selection of samples

Only undisturbed surfaces of the uppermost sediment layer (no fluff layers) were included in the study. Sampling was done either by a giant box corer, a multicorer, or a so-called minicorer (a small sampling device that can be placed below a rosette of Niskin bottles). No data from gravity corer or piston corer samples were accepted, because the preservation of the sediment surface may be poor for these sampling methods. The dataset was based on existing data of $^{230}Th_{ex}$ [*Walter et al.*, 1997]. Further analyses of ^{230}Th were performed on samples where large gaps in the spatial distribution of sample locations were found. If not yet measured, biogenic opal was analysed in samples where ^{230}Th data were available. Existing sample material as well as additional information could be identified by means of the PANGAEA database (http://www.pangaea.de). Five samples had to be excluded from the investigation after analysis. Two samples in the vicinity of the South Sandwich Islands (PS

2292-1, PS2293-1) turned out to contain substantial amounts of volcanic glass, which led to an overestimation of the opal content. Two more samples (PS63/121-2 and PS63/136-2) were excluded when smear-slides of the sediment revealed a contribution of microfossils from the tertiary period. This is a case of post-depositional sediment redistribution, which would obscure the original ^{230}Th-signal [*François et al.*, 2004]. One more sample (PS63/141-2) had to be excluded because both ^{232}Th and ^{230}Th were a factor 5-10 higher than in all surrounding samples, probably due to a large contribution from a manganese concretion in the sample. Stations shallower than 1000 m are not included in this study, because they definitely represent shelf or continental margin areas, which deserve a different approach.

The dataset is available online (http://doi.pangaea.de/10.1594/PANGAEA.230042).

2.2 Measurement of biogenic opal

The reported values for biogenic opal were obtained by two different methods, both based on the dissolution of biogenic opal in alkaline media. A part of the samples was processed by sequential dissolution with 2 M Na_2CO_3 (pH 12.5) at 85°C, and corrected for clay contributions according to *DeMaster* [1981]. Part of these data were published earlier [*Schlüter et al.*, 1998]) and are available online (PANGAEA). This method is particularly suitable for samples with low opal content [*Schlüter and Rickert*, 1998] as observed in the Weddell Sea. The other part of the samples was analysed by dissolving biogenic silica in 1 M NaOH according to *Müller and Schneider* [1993]. Contributions of lithogenic silica were identified by monitoring the dissolution vs. time, and appropriate corrections were applied. The dissolution in 1 M NaOH may lead to an overestimation of the values for low opal contents (<10%), but it yields comparable results for higher opal contents [*Schlüter and Rickert*, 1998]. Some available data on opal content based on X-ray diffraction have been excluded in this study, because correlation with wet-chemical extraction data (when available) was poor, as described for reference materials in *Conley* [1998]. Both wet-chemical methods

are appropriate techniques to analyse marine sediments with a certain opal content, avoiding partial dissolution by means of a strongly alkaline medium, and correcting for silica contributions from clay.

2.3 Measurement of $^{230}Th_{ex}$

Thorium-230 in excess of its progenitor ^{234}U ($^{230}Th_{ex}$) is derived from production in the water column. For the analysis of $^{230}Th_{ex}$ by means of α-spectrometry, 0.2-0.5 g of ground sample were spiked with appropriate amounts of yield tracer (^{229}Th, ^{236}U), and digested completely. After separation and purification of the nuclides, Th and U were electroplated onto silver discs, and the activities of the nuclides were determined by α-counting. For the calculation of $^{230}Th_{ex}$, the fraction of ^{230}Th in equilibrium with its progenitor ^{234}U from terrestrial input (supported ^{230}Th) has to be subtracted from bulk ^{230}Th. In most cases, supported ^{230}Th could be assumed to be in equilibrium with ^{234}U, and $^{230}Th_{ex}$ was calculated as the difference between ^{230}Th and ^{234}U. In some cases, evidence for some authigenic ^{234}U was found ($^{234}U/^{232}Th$ ratio exceeding 0.8). In these cases, supported ^{230}Th was calculated from the natural $^{234}U/^{232}Th$ ratio in the sediment, which was assumed to be 0.4. More details about this procedure are given in *Walter et al.* [1997]. In cases with very low ^{230}Th activities, this correction may change the final value of $^{230}Th_{ex}$ up to 25%. Most of the values that were affected by authigenic Uranium only changed insignificantly by about 5%. The given 1 σ-errors are derived from counting statistics. They include error propagation and the error of the blank correction.

2.4 ^{230}Th-corrected opal accumulation rates

The naturally occuring radionuclide ^{230}Th used for the calculation of vertical fluxes here is a decay product of ^{234}U. Uranium is displaying a conservative behavior under most oceanic conditions, and its concentration in the ocean is closely coupled to salinity. The production of

^{230}Th by decay of ^{234}U in the seawater is a simple function of Uranium activity and the decay constant λ of ^{230}Th (λ = 9.2174*10^{-6}*yr^{-1}), and as the Uranium concentration is well constrained, the annual production of ^{230}Th (β) in seawater can be calculated to be 0.026 dpm*m^{-3}*yr^{-1} for salinities around 34.5, like typically observed in most of the Southern Ocean. Consequently, the integrated production of ^{230}Th in the water column overlying an area of one square meter of sea floor is the product of β and the water depth z [m]. Assuming that the particle reactive ^{230}Th reaches the sediment via particle flux completely at the production site, the estimated ^{230}Th flux (F_{Th}) to the sediment surface is

$$F_{Th} = \beta * z \tag{1}$$

This fraction of ^{230}Th exceeding the secular equilibrium with ^{234}U found in deep-sea sediments, received from the overlying water column, is known as excess ^{230}Th or ^{230}Th$_{ex}$. This well known constant flux of ^{230}Th$_{ex}$ to the sediment has repeatedly been used to identify sites of sediment redistribution, to calculate sediment accumulation rates or to quantify the fluxes of individual sedimentary components [e.g. *Suman and Bacon* 1989, *François et al.*, 1993, *Thomson et al.*, 1993, *Frank et al.*, 1999, *François et al.*, 2004). Based on the constant flux of ^{230}Th$_{ex}$, the preserved vertical flux of any sedimentary component i can be expressed as

$$^{pr}F_v^i = \frac{\beta * z * f_i}{[^{230}Th_{ex}]_0} \tag{2}$$

where $^{pr}F_v^i$ is the preserved vertical flux of component i (e.g. biogenic opal) in [g*m^{-2}*yr^{-1}], β is the production rate of ^{230}Th in the water column [dpm*m^{-3}*yr^{-1}], z is the water depth [m], f_i is the weight fraction of component *i*, and $[^{230}Th_{ex}]_0$ is the specific activity of ^{230}Th in the sediment at the time of deposition, exceeding the activity of ^{234}U [dpm*g^{-1}].

By restricting the approach here to recent sediment surfaces, we can neglect the decay of ^{230}Th. This makes an independent determination of the age unnecessary.

If we set f_i to unity, the equation gives the vertically received, preserved mass flux for the sum of all sedimentary components ($^{pr}F_v^{tot}$).

$$^{pr}F_v^{tot} = \frac{\beta * z}{[^{230}Th_{ex}]} \tag{3}$$

When normalizing the flux of a sedimentary component to the flux of Thorium, we implicitly also correct for lateral sediment redistribution. Assuming that the laterally redistributed sediment is identical to the vertically deposited sediment with respect to its content in Thorium and the sedimentary component to be investigated, we introduce no bias into the flux calculation when receiving lateral inputs. Thus, the equation is a comparably simple way to convert weight fractions of a sedimentary component together with $^{230}Th_{ex}$ activities into fluxes of the respective component. However, several implicit assumptions are made when applying this model, which are not necessarily met. The following section will give an overview of the implicit assumptions, the consequences of their potential violation and how we exclude, encounter or quantify the error introduced into our opal fluxes this way.

2.4.1 Potential errors in the normalization procedure

When discussing the potential errors introduced by the ^{230}Th normalization, two facts should be kept in mind. First, there is in most cases no other way to determine vertical fluxes into the sediment. Second, if fluxes based on sediment dating are available, and focusing and winnowing remain ignored, errors may easily bias the data by a factor up to 12 in the ACC [*Frank et al*., 1999].

We have to account for three potential error sources in our normalization procedure:

-Post-depositional sediment redistribution

-Selective lateral transport of sedimentary components bearing differing $^{230}Th_{ex}$ signals

-Advection of ^{230}Th in the water column

Post-depositional sediment redistribution means the presence of old sediments in the sample, in which part of the $^{230}Th_{ex}$ has decayed. This might be either a consequence of lateral inputs

of old sediments remobilized by erosion, or the sample itself might be of older age due to erosion at the sampling site or inappropriate sampling (e.g., analysis of core tops with missing surface). In our case, the latter was excluded by using only the very surface of Multicorer samples, which have largely undisturbed surface layers. This is of particular importance because particle fluxes are known to have varied considerably even during the Holocene period. More problematic would be a lateral contribution of old sediments poor in $^{230}Th_{ex}$, which would be taken for recent vertical fluxes by the ^{230}Th constant flux model. Such a redistribution of old sediment would be expected when the conditions of sedimentation, i.e. the near-bottom ocean circulation, are subject to a substantial change. At least for the Late Holocene, which our samples do represent, we do not expect such changes. Therefore, we consider our results to be unbiased by age effects. An exception might be the Argentine Basin, where slowly migrating mudwaves at the deep-sea floor might uncover older sediments. In the Eastern Weddell Gyre, two samples had to be discarded because contributions of non-recent sediments were identified.

Selective lateral transport of sedimentary components bearing different $^{230}Th_{ex}$-signals (sorting) was one of the main concerns when applying $^{230}Th_{ex}$ for flux calculations [*François et al.*, 2004], because different particle types have different affinities for Thorium, depending on their size and composition (*Thomson et al.*, 1993; *Chase et al.*, 2002, 2003; *Geibert and Usbeck*, 2004). Implicitly, our model assumes that the $^{230}Th_{ex}$ fraction found on a distinct particle type corresponds to the mass fraction that it represents. This assumption is obviously not fully met. However, the results of *Thomson et al.* [1993] have shown that $^{230}Th_{ex}$ activities in the different size fractions do not differ by more than a factor two, excluding only the largest lithogenic particles. Consequently, *François et al.* [2004] recommend not to use the ^{230}Th-normalization for particles as large as ice-rafted debris or large single foraminifera, while the use for smaller particles, representing the bulk of marine sediments, will not introduce additional bias into the data.

Advection of ^{230}Th in the water column is an effect that has to be taken into account in a strongly dynamic area like the Southern Ocean. Here, rapid exchange of water masses between different basins and strong contrasts in particle flux may occur. However, the so-called boundary scavenging effect, leading to increased scavenging in regions of high particle flux and vice versa, has been shown to be comparably weak for Thorium [*Henderson et al*., 1999]. According to the modeling studies of *Henderson et al.* [1999], about 70% of the ocean floor can be assumed to receive a Th flux within 30% of that expected from production. These findings were confirmed by measurements [*Yu et al.*, 2001], showing that ^{230}Th fluxes are typically found within a narrow range around the water-column production. A known exception to the commonly small deviation of ^{230}Th flux from the water column production is the Western Weddell Gyre. There, $^{230}Th_{ex}$ inventories in deep-sea sediments as well as sediment trap data have shown that only about 40% of the ^{230}Th production reaches the deep-sea floor [*Walter et al.*, 2000].

Because the deviation of ^{230}Th flux in the Weddell Gyre is well constrained, we include it in our calculations as a correction factor. These data (for the definition of the regions, see Figure 5 and corresponding text below) have been adjusted, assuming that ^{230}Th-fluxes are 40% of the expected ^{230}Th-production [*Walter et al.*, 2000]. This correction results in a decrease of the calculated opal fluxes in the Weddell Gyre by factor 2.5. The correction has been applied to the Eastern part of the Weddell Gyre, too, in order to avoid a discontinuity in the data, although it is not clear whether the adjustment should be the same for this region. This should be kept in mind when considering the calculated fluxes in the Eastern Weddell Gyre. The ^{230}Th not scavenged in the Weddell Gyre must be expected to be buried in the ACC [*Walter et al.*, 2000]. However, it is unclear over which area this potential ^{230}Th input is spread, as current speeds in the ACC are high, and mixing is intense. Currently, we cannot localize this input of ^{230}Th, and the deviation from the expected ^{230}Th-flux should be found within the 30% error given by *Henderson et al.* [1999]. Therefore, we did not apply any additional correction

for advective inputs here. For the other investigated areas, there is no reason to expect unusual deviations from ^{230}Th production patterns. The Weddell Gyre remains the only region for which we applied a correction for advective losses in ^{230}Th.

After having corrected the fluxes for the Weddell Gyre, and leaving the values for the other regions unchanged, we estimate the error introduced to the calculated fluxes by ^{230}Th advection in the water column to be within the 30% range given by *Henderson et al.* [1999]. Other errors can be assumed to be contained within that range, and further diminished by eventually considering mean values for whole regions, composed of several samples. The obtained data represent a considerable progress to uncorrected flux data, and provide currently by far the best estimate of opal fluxes to the sediments of the Atlantic sector of the Southern Ocean.

2.4.2 What do the Th-normalized opal fluxes mean?

Thorium-normalized fluxes have been reported in the literature under a variety of names. They have been called vertical rain rates [*Frank et al.*, 2000], ^{230}Th-normalized burial flux [*Sayles et al.*, 2001]), or ^{230}Th-normalized accumulation rates [*Pondaven et al.*, 2000]. Each of these names has its individual shortcomings for our case. The term "rain rate" might be confounded with the flux arriving at the sediment. "Burial flux" implies that the given flux is actually completely buried, which does not necessarily apply to our case (surface sediments). "Th-normalized accumulation rate" bears the risk to be confounded with accumulation rates derived from Th-dating, like they have been provided by *DeMaster* [1981]. We therefore decided to adopt the term "preserved vertical flux" ($^{pr}F_V$), as defined by *François et al.* [2004].

The values presented here are not identical with vertical opal rain rates to the sediment, as the upper cm of the sediment may have been subject to some dissolution after opal deposition. An imaginary sediment trap directly above the sea floor would catch higher particle fluxes than

what we find back in the uppermost sediment, as directly shown by *Sayles et al.* [2001]. Estimates of the silica dissolution that is taking place between the recent sediment surface and the actually buried sediment from the Indian sector of the Southern Ocean indicate that actual burial fluxes will reach about 40-70% of the preserved vertical flux in the upper cm ("dissolution-corrected opal rain rate" in the reference) [*Dezileau et al.,* 2003]. Therefore, our values are a lower limit for opal rain rates to the sediment, and an upper limit for opal burial rateswhich they should closely approach. Thus, our Th-normalized preserved vertical fluxes are suitable to calculate spatial budgets or to be used in modelling studies.

3 Results

3.1 Biogenic opal concentrations

The opal contents displayed in Figure 1 range from close to zero to about 80 %. Biogenic opal contents >30% are indicated by reddish colors in Figure 1. Their occurrence is restricted to the southern part of the ACC.

In the Atlantic Sector, the southern boundary of siliceous deposits is matched best by the Southern ACC boundary. The adjoining area towards the South, the Weddell Gyre, is characterized by very low contents of biogenic silica that slightly increase towards the East, neglecting some exceptions near Maud Rise (66°S, 3°W). The limit of the maximum northern sea-ice extent (15% ice cover in August according to Comiso 2003) does not coincide exactly with the southern boundary of silica-rich deposits in the Atlantic sector. Siliceous ooze still occurs south of this boundary. The northern boundary of the occurrence of siliceous ooze in the Atlantic is matched fairly well by the position of the APF, considering that the front is actually not a stationary feature, but moving across several degrees of latitude [*Moore et al.*, 1999]. This does not hold true for the Pacific sector, where siliceous ooze is found considerably north of the APF.

The two longitudinal sections in the Pacific Sector differ clearly in their biogenic opal content. Whereas the surface sediments of the western section have opal contents exceeding 60%, the eastern section only reaches values around 20%. The few samples from the Indian Sector indicate a southward shift of the opal belt compared to the Atlantic sector, in accordance with the frontal system of the ACC.

3.2 $^{230}Th_{ex}$

The distribution of $^{230}Th_{ex}$ reveals clear spatial patterns in the area of investigation. Lowest values are found in the Atlantic sector, especially in the Southern ACC. In the Weddell Gyre, ^{230}Th values are higher than in the Southern ACC, with a tendency to increase eastwards. Values north of the APF are consistently higher than south of this boundary, comparable with those in the Weddell Gyre.

In the Pacific Sector, two major regimes of ^{230}Th in surface sediments are seen. Whereas most unsupported ^{230}Th activities are in the range between 20 and 30 dpm/g, the region north of the APF around 90°W has substantially higher activities, from 50 to 90 dpm/g. These are the highest values in our area of investigation.

3.3 Preserved vertical sediment fluxes

Combining the information from $^{230}Th_{ex}$ with the depth of the overlying water column, total vertical sediment fluxes ($^{pr}F_v^{tot}$), corresponding to Th-normalized bulk sediment accumulation rates, can be derived (see Figure 3, calculation as given in paragraph 2.4). Lowest $^{pr}F_v^{tot}$ are found in the Eastern Weddell Gyre, and in the Northern ACC in the Southeast Pacific sector. For the Eastern Weddell Gyre, there is some uncertainty in the data, as they were corrected for Th-advection, which has so far only been constrained for the Western Weddell Gyre. Actual values might be higher up to a factor 2.5 (assuming no advective loss of ^{230}Th). Maximum values for the $^{pr}F_v^{tot}$ are found in the Southern ACC in the Atlantic and Indian

sector, with several values exceeding 25 $g*m^{-2}*yr^{-1}$ but no value exceeding 32 $g*m^{-2}*yr^{-1}$. Most open ocean values far from terrestrial sources are found in a narrow range between five and 15 $g*m^{-2}*yr^{-1}$.

3.4 Preserved vertical silica fluxes

Preserved vertical silica fluxes ($^{pr}F_v^{Si}$) are obtained from combining biogenic opal concentrations and $^{230}Th_{ex}$-activities. Some areas with comparably high opal concentrations are found to receive low silica fluxes, like the Northern ACC in the Southeast Pacific sector. The Southern ACC in the South Pacific, South Atlantic, and Indian Sector is clearly identified as the region of maximum opal fluxes to the sediment in our area of investigation.

Regions of differing opal fluxes can be distinguished in the new map of vertical fluxes of biogenic opal (Figure 4). Based on this picture, areas of consistent opal sedimentation can be selected. These consistent regions will serve us as a reference to calculate budgets for distinct regions of the Southern Ocean.

3.5 Calculating regional budgets

3.5.1 Selecting consistent regions

The calculation of regional budgets requires appropriate definitions of sufficiently homogenous regions. Besides homogeneity, two further properties of the regions are required: they should reflect classical definitions of ocean basins (e.g. “Atlantic”), and some oceanographic features playing a major role in silica distribution have to be considered. Earlier works on silica fluxes have selected regions according to the silica distribution in sediments based on the original dataset of *Cooke and Hays* [1982], or they were following the classical separation of regions by their respective sea-ice distribution [*Tréguer and van Bennekom*, 1991] into the Polar Front Zone (PFZ), the Permanently Open Ocean Zone

(POOZ), and the Seasonal Ice Zone (SIZ). Here, we follow the latter approach for reasons of comparability, although we acknowledge that many other factors besides sea-ice may control silica production and preservation [*Ragueneau et al.*, 2000]. *Tréguer and van Bennekom* [1991] have pointed out mainly the role of sea-ice, being coupled to nutrient distribution by the underlying oceanography. Other works have demonstrated the role of temperature in controlling silica production in the Northern ACC [*Burckle and Cirilli*, 1987]), and recently, the distribution of the growth-limiting micronutrient iron has been shown to be another important influence on silica production [*de Baar et al.*, 1995]. As our work is focusing on silica fluxes, we have chosen this parameter to define regions (see Figure 5).

The boundaries found in silica fluxes do not always exactly match the boundaries of the classical regions Polar Front Zone (PFZ), Permanently Open Ocean Zone (POOZ), and the Seasonal Ice Zone (SIZ) according to *Tréguer and van Bennekom* [1991]. However, differences are small enough to adapt the definitions of *Tréguer and van Bennekom* [1991] to our study, thus facilitating a comparison with other data.

It should be noted that we summarize the PFZ and the SAZ to one regime, which comprises the whole ACC north of the Polar Front because we find no substantial difference between the two regions in terms of opal fluxes. Concerning the POOZ, we set the APF as its northern boundary. Its southern boundary is marked in the data by a sharp gradient in vertical silica fluxes, which is found in between the maximum sea ice extent (15 % sea-ice cover in August according to *Comiso* [2003] and the Southern ACC boundary [*Orsi et al.*, 1995]. The Eastern and Western Weddell Gyre are not called SIZ here, although this would seem appropriate from their sea-ice distribution. In terms of silica preservation, the Weddell Gyre is so different from other regions with seasonal ice cover (*Leynaert et al.*, 1993; *Zielinski and Gersonde*, 1998; *Usbeck et al*., 2002) that it should be considered separately.

The longitudinal boundaries have mainly been chosen according to classical definitions of ocean basins (International Hydrographic Organization IHO, after *Tomczak and Godfrey*

[1994]). An additional longitudinal boundary has been placed between the South Pacific and the Southeast Pacific region, because clear differences are found there in terms of vertical silica rain rates.

The Weddell Gyre is divided here into two separate regions, with a boundary at 10°W. The reasons for this separation are higher silica contents in sediments of the Eastern Weddell Gyre compared to the western domain, model results suggesting a different productivity regime [*Usbeck et al.*, 2002], and preliminary results of an expedition to the Eastern Weddell Gyre, suggesting considerable biogenic silica production at 23°E [*Geibert et al.*, 2004]. The eastern boundary of the Weddell Gyre is following the Southern ACC boundary instead of the Atlantic/Indian sector boundary. We count this area as belonging to the Atlantic Sector, because we want to avoid the division of a consistent region in two. The calculated surface area of the Atlantic Sector remains largely unaffected by this exception.

We explicitly exclude shelf areas from our consideration, because the $^{230}Th_{ex}$-normalization is not suitable in that simple form for shallow oceanic regions [*François et al.*, 2004]. In some cases, the calculation of surface areas was not possible because it was not clear for which area the samples were representative (regions 5, 6, 7).

3.5.2 Th-normalized sedimentation data in the regions

Regional budgets and mean values for ${}^{pr}F_v^{tot}$, biogenic silica content and ${}^{pr}F_v^{Si}$ are given in Table 1. For some samples, the Th-content was available, but not the biogenic silica content, and vice versa. This explains the differing sample numbers given for the respective variables. Consequently, the mean silica flux cannot be calculated from a mean Th-content and a mean biogenic silica content for the regions. Instead, the mean silica flux is calculated from all individual samples for which both $^{230}Th_{ex}$ and biogenic silica content were available. The surface area of the regions is given in cm^2 in order to facilitate a comparison with earlier publications [*DeMaster*, 1981; 2002]. Shelf areas are excluded, as shown in Figure 5.

The meaning of the given errors for the individual parameters deserves an explanation. The calculation of a standard deviation usually requires a sufficient sample size and a normal distribution of the values around the mean value. Especially the latter assumption is not met in our case. A more precise error calculation would require fitting a different frequency distribution model to the data. However, our sample size is too small to select an appropriate distribution. Considering the skewness of the data distribution in a qualitative way, we conclude that the true error of the mean will be smaller than the standard deviation to the lower side of the values, and larger to the greater side. We chose to give the standard deviation based on a normal distribution in spite of these obvious problems, because the concept of the standard deviation is well known, and it has been used in earlier publications.

Having a closer look at the silica budgets in the Atlantic Sector, we find that the open Weddell Gyre is a minor sedimentary sink for biogenic silica. The POOZ in the Atlantic Sector is representing 67 % of the silica budget in the Atlantic, followed by the PFZ and SAZ that account together for another 29 %. Although the error of 33 % in the total Atlantic budget may seem to be large, it is much smaller than in previous works, and the small standard

deviation within the regions indicates that the selected areas are internally consistent. Summarizing the obtained silica budgets, we can state that from 112°W to 20°E, the flux of biogenic silica into the sediments of the Southern Ocean is 4.6 ± 1.5 *10^{11} mol/yr.

4 Discussion

4.1 Distribution of biogenic silica in surface sediments

The map of biogenic opal concentrations reveals some major differences to the hitherto used reference map from *DeMaster* [1981] and *DeMaster* [2002], as well as to the contrasting map of *Lisitzin* [1985]. For the Atlantic sector, the band of maximum siliceous ooze deposits can be found in the POOZ, with a mean opal content of 31 ± 14 % (n=40). Lower opal contents are found north of the APF in the PFZ, which is in agreement with the depletion of silica in surface waters north of approximately this location. However, no maximum of opal contents (or vertical silica fluxes) can be found in the vicinity of the APF as reported earlier [*DeMaster et al.*, 1991]. In contrast to the southern boundaries of the opal belt of DeMaster, opal contents in the Western Weddell Gyre are observed to be consistently low. The gap in highly siliceous deposits east of about 30°W in the Scotia Sea according to DeMaster can be shown to be non-existent, as reported by *Zielinski and Gersonde* [1997] and *Schlüter et al.* [1998]. A number of samples from the Scotia Sea near the Weddell-Scotia Confluence are found to contain considerable amounts of biogenic silica, and 3 samples west of 30°W and North of 55°S also have elevated opal contents [*Schlüter et al.*, 1998]. In this region, our data agree better with the map of *Lisitzin* [1985].

In the Southeast Pacific, two contrasting longitudinal sections of sediment surface opal contents are available. The eastern section has opal contents comparable to Atlantic sediments. In contrast to the Atlantic Sector, the PF does not coincide with the northern limit of the opal belt here. High contents of biogenic silica are found north of the position of the

APF. The highest opal contents of all included samples were measured in the western section from the Southeast Pacific at about 120°W.

A comparison with the map of *Lisitzin* [1985] is more difficult, because he only gives opal content in the carbonate-free sediment, whereas we consider the fraction of dry bulk sediment. The most prominent difference to our data is found in the Weddell Gyre, where we found virtually no biogenic opal in the western part, whereas the map of Lisitzin would let us expect values of 10-50% opal for this region, which cannot be explained by carbonate in the samples. A comparison is difficult, too, because the actual sample locations leading to the establishment of the boundary of the opal belt are not marked in the maps of Lisitzin [1985] or DeMaster [1981, 2002].

Summarizing our findings concerning the distribution of biogenic silica contents in the Atlantic sector, we find significantly lower values than previously reported: 31 ± 14 % in the POOZ, and 14 ± 9 % in the PFZ and SAZ, compared to 55 ± 10 % [DeMaster 1981]. The main area of silica deposition has boundaries that differ considerably from earlier maps. The core of the Atlantic opal belt is found to be the POOZ, covering an area of just $4.6*10^{16}$ cm^2.

4.2 Bulk vertical fluxes and estimates of focusing-corrected sedimentation rates

The mean preserved bulk vertical fluxes ($^{pr}F_v^{tot}$) are found in a surprisingly narrow range from 2.9 $g*m^{-2}*yr^{-1}$ (in the Eastern Weddell Gyre) to 15.8 $g*m^{-2}*yr^{-1}$ (POOZ Indian Sector). Assuming a mean dry bulk density of 0.4 $g*cm^{-3}$ for the band of highly siliceous sediments in the Southern ACC [DeMaster 1981], we can estimate mean normalized sedimentation rates of 4 $cm*kyr^{-1}$ for the Indian sector and 3.5 $cm*kyr^{-1}$ for the Atlantic sector. Comparing these normalized data to uncorrected values for sedimentation rates, an impression of the bias towards high sedimentation rates by selective sampling can be given. *DeMaster* [1981] found the mean sedimentation rate in the South Atlantic to be 16.8 $cm*kyr^{-1}$. This compares to 3.5 $cm*kyr^{-1}$ in our case which includes the correction for sediment redistribution. In all the

analysed material from the open Southern Ocean, we found no normalized vertical flux that would correspond to a sedimentation rate of more than 10 cm*kyr^{-1}.

4.3 Vertical silica fluxes compared with earlier results

When comparing our results to those of other investigators, we must separate focusing-corrected data from uncorrected ones. The extent of the difference between the two data types depends on the degree of sediment redistribution in the respective regions. To give an example, we compare the difference of corrected and uncorrected values in the Western Weddell Gyre with the respective differences in the ACC. Sediments in the deep-sea of the Western Weddell Gyre far off the coast seem to be largely unaffected by sediment redistribution [*Walter et al.*, 2000], whereas sediments underlying the ACC are strongly affected by focusing and winnowing [*Frank et al.*, 1999]. Consequently, results for uncorrected and corrected data do not differ much in the Western Weddell Gyre (*Schlüter et al.* [1998]: 0.17-1.3 mmol*m^{-2}*yr^{-1} versus 0.7 ± 0.1 mmol*m^{-2}*yr^{-1} in our work). In contrast, differences are very high in the Atlantic sector of the ACC (*Schlüter et al.* [1998]: 367-380 mmol*m^{-2}*yr^{-1} versus 61 ± 29 mmol*m^{-2}*yr^{-1} in our work).

Comparing our preserved vertical flux to Th-normalized data of *DeMaster* [2002] from the Atlantic sector, we obtain considerably lower values. *DeMaster* [2002] gives a Th-corrected mean of 167 ± 146 mmol*m^{-2}*yr^{-1} (n=9) for the region considered to accumulate siliceous ooze in the Atlantic sector. This value should compare to our region 2 (POOZ Atlantic), receiving the highest fluxes. For this region, we calculate 61 ± 29 mmol*m^{-2}*yr^{-1} (n=31). Although our value is not outside the error range given by DeMaster, it changes considerably the understanding of the importance of the Atlantic Sector of the Southern Ocean as a major sink for silica, especially when considering the necessary adjustment in the spatial extent of the area that is covered by siliceous sediments.

Better agreement is found with Th-normalized data from the other sectors (see Table 2). *Pondaven et al.* [2000] give Th-normalized silica accumulation data for a transect along 62°E (ANTARES section), separately for the PFZ and the POOZ. Additional data from the Indian sector (six values from gravity cores for the marine isotope stage 1 from about 73°E to 110°E) are available from *Dezileau et al.* [2003]. For the PFZ in the Indian sector, 75 ± 42 mmol*m^{-2}*yr^{-1} [*Pondaven et al*., 2000], or 10, 17, 35 and 12 mmol*m^{-2}*yr^{-1} [*Dezileau et al.*, 2003] compare to two individual values from our work (PS2562 and PS2611): 14 and 18 mmol*m^{-2}*yr^{-1}, which we consider as a reasonable agreement. For the POOZ in the Indian sector, *Pondaven et al.* [2000] give 210 ± 40 mmol*m^{-2}*yr^{-1}, and *Dezileau et al.* [2003] find 216 and 297 mmol*m^{-2}*yr^{-1}. We can compare three individual values from the POOZ of the Indian Sector to these data (PS63/149, PS63/146, PS2604; two samples located in the Seasonal Ice Zone have to be excluded for better comparability): 191, 151, and 82 mmol*m^{-2}*yr^{-1}. Considering the differing sampling sites and sampling techniques (gravity corer vs. multicorer), this is again a reasonable agreement.

In the Pacific Sector, the AESOPS section at 170°W is another good comparison to our data, as the underlying Th-normalization is given in detail [*Sayles et al*., 2001]. For the POOZ at 170°W, the burial fluxes reported by *Sayles et al.* [2001] corresponding to our Th-normalized fluxes range from about 89 to 273 mmol*m^{-2}*yr^{-1}. Our region 7, consisting mainly of a section at about 115 °W, receives a mean flux of 50 ± 21 mmol*m^{-2}*yr^{-1}. For the PFZ at 170°W, *Sayles et al.* report fluxes of about 8-50 mmol*m^{-2}*yr^{-1}. We have no data for comparison in the same ocean basin for the PFZ.

Our mean values for the Atlantic are considerably lower than the mean values in the Indian sector (ANTARES section), or than the AESOPS data from the Pacific. In the POOZ of the Atlantic Sector we find a preserved vertical silica flux of 61 ± 29 mmol*m^{-2}*yr^{-1}. This compares with 210 ± 40 mmol*m^{-2}*yr^{-1} of *Pondaven et al.* [2000] in the Indian Sector, and with 100-300 mmol*m^{-2}*yr^{-1} for the Pacific sector [*Sayles et al.*, 2001]. Our studies include

two regions in the Weddell Gyre that have so far not been subject to studies with Th-normalized silica fluxes. It is worth mentioning the exceptionally low fluxes (mean values: 0.7 ± 0.1 mmol*m^{-2}*yr^{-1} in the western part and 6.3 ± 3.2 mmol*m^{-2}*yr^{-1} in the eastern part) that are in contrast with the observed productivity. *Leynaert et al.* [1993] report an annual biogenic silica production of 810-870 mmol*m^{-2}*yr^{-1} in the northern Weddell Gyre. Recent studies could remove many of the apparent contradictions between different regions in opal preservation [*Pondaven et al.* 2000; *Nelson et al.* 2002], but the poor preservation in the Weddell Gyre, already found by other investigators (*Leynaert et al*., 1993; *Zielinski et al.,* 1998; *Usbeck et al*., 2002), remains an unsolved problem.

In a circumantarctic view, it turns out that the regions of high biogenic opal fluxes are found in the POOZ, located in between the Southern Boundary of the ACC and the APF. The PFZ does clearly accumulate less silica than the POOZ. The APF itself is not found to support high silica fluxes, but only to designate the northern boundary of the opal belt in the Atlantic and Indian sector. In contrast to the findings of *DeMaster* [2002], we can show significant differences between ocean basins, and clear spatial patterns are found in silica fluxes to the sediment in the Southern Ocean.

The normalized values for silica accumulation in the sediment as provided here resolve some apparent inconsistencies between rain rates in the water column and the flux into the sediment in the Southern Ocean [Pondaven et al. 2000; Ragueneau et al. 2000]. A compilation of silica fluxes from various regions provided by Raguenau et al. [2000] had reported a close agreement between calculated silica fluxes into the sediment (burial + recycling term) and measured rain rates to the seafloor, except for the Southern Ocean (Indian Sector). Here, calculated fluxes to the sediment that were based on silica distribution in porewater were exceeding the measured rain rates several times. The Th-normalized fluxes into the sediment that we have obtained now are considerably lower than the measured rain rates reported by

Ragueneau et al. [2000], indicating a reasonable order of magnitude of silica accumulation in the Southern Ocean if we account for focusing.

4.4 Regional budgets: quantifying the opal belt

Our estimate for silica flux into the sediments of the Atlantic sector of the Southern Ocean is $4.2*10^{11} \pm 1.4*10^{11}$ mol*yr^{-1} (see Table 1). The Th-normalized value for comparison is given by *DeMaster* [2002], with $8.6 * 10^{11}$ mol*yr^{-1} for this region. We reduce this estimate by one half. It is worth noting that *DeMaster* [2002] excludes "erosional areas", and that the surface area he integrates into the study is therefore only $0.5*10^{17}$ cm^2, whereas we include a surface area of $1.8 * 10^{17}$ cm^2. If we only compare region 2 (POOZ Atlantic Sector), having a surface area of $0.46*10^{17}$ cm^2, to the opal belt of *DeMaster* [2002] in the Atlantic, we come up with an estimate of $2.8 \pm 1.3*10^{11}$ mol/y, just one third of the previous estimate.

The reason for this difference can in part be seen in the larger number of samples in our study (70 stations in the Atlantic sector, compared to nine stations in DeMaster's work). However, some need for explanation remains, considering that three stations out of nine in *DeMaster* [2002] display vertical silica fluxes exceeding 300 mmol*m^{-2}*yr^{-1}, whereas our highest value in the whole Atlantic is found to be 140 mmol*m^{-2}*yr^{-1}. Going back into the underlying methods of the original data of *DeMaster* [2002] [*Frank*, 1996; *François et al.*, 1997], a possible explanation would be the use of biogenic opal values obtained by XRD-measurement (X-ray diffraction), or from gravity or piston cores. While the XRD method has been successfully applied to down-core variations [*Frank*, 1996], it is doubtful whether it can be applied for absolute opal determinations at the sediment surface. A comparison with wet chemical methods [*Conley*, 1998] has revealed that higher values may be obtained by the XRD method, especially for high opal contents of the sample. Surface sediments with their high porosity and consequently high sea-salt content are especially challenging for XRD-measurements. A factor of two difference in the silica content can in this case easily be a

result of the differing methods. As we have excluded both opal data obtained by XRD as well as samples from gravity and piston cores, these samples were not included in our study.

The current best estimate for silica output from the world ocean is $7.1 \pm 1.8\ 10^{12}$ mol*yr^{-1} [*Tréguer et al.*, 1995]. Our correction of the silica fluxes in the Atlantic sector of the Southern Ocean would lead to a reduction of 6% of this global output term. Although this reduction is still contained in the error estimate of *Tréguer et al.* [1995], our result raises the question whether values for the other ocean basins are not overestimated, too, as sediment redistribution has largely been ignored in earlier works.

The existence of focusing and winnowing and the resulting need for high spatial resolution or normalization in budget studies has been clearly demonstrated by other approaches than ^{230}Th normalization as well [*Mollenhauer et al.*, 2002], and this effect is by no means restricted to the Southern Ocean. This area with its high current speeds is certainly a place with particularly strong bottom currents, favouring the occurrence of sediment redistribution. However, sediment redistribution is a global phenomenon, and the main cause for previous overestimations of vertical fluxes to the sediment must be seen in selective sampling at sites of high accumulation rates. The effect will be more pronounced in the Southern Ocean, but the trend overestimate fluxes from sediment cores will persist in other ocean basins as well, if no correction is applied.

5 Summary and outlook

Our work has made several steps towards a better quantification of fluxes to the sediment in the marine environment. These steps consist in a restrictive sample selection, an improved spatial resolution, and the consequent application of ^{230}Th as a tool for correction of the influence of sediment redistribution, including known restrictions of the underlying model assumptions.

For the Atlantic sector of the Southern Ocean, our new dataset has reduced the expected burial flux of biogenic silica to the sediment by one half compared to earlier estimates [*DeMaster*, 2002]. A comparison to Th-normalized data from other regions of the Southern Ocean has shown that the Atlantic sector is accumulating less silica than comparable regions in the Indian or Pacific sector. Different provinces of sediment accumulation could be derived by the improved spatial resolution, thus leading to new estimates for the surface area covered by distinct types of sediment.

The strong shift in the data when applying an appropriate correction for sediment focusing has implications for flux estimates of other sedimentary components, too. In particular, fluxes of carbonate, organic carbon, and terrigeneous components could be much better constrained by a comparable ^{230}Th-normalized dataset. This will not only improve our understanding of current biogeochemical cycles, but also give us the tool to develop models for past situations on a quantitative level.

Acknowledgements

We thank Ingrid Vöge for doing a great job in the Th analysis. Gerhard Fischer generously provided data of biogenic opal contents.

References

Bacon, M.P. and J. N. Rosholt (1982), Accumulation rates of ^{230}Th, ^{231}Pa, and some transition metals on the Bermuda Rise, *Geochim. Cosmochim. Acta*, *46*, 651-666.

Burckle, L.H., D. Robinson, and D. Cooke, (1982), Reappraisal of sea-ice distribution in Atlantic and Pacific sectors of the Southern Ocean, *Nature*, *299*, 435-437.

Burckle, L.H. and J. Cirilli (1987), Origin of diatom ooze belt in the Southern Ocean: Implications for late quaternary paleoceanography, *Micropaleontology, 33 (1)*, 82-86.

Broecker, W.S. and T.-H. Peng (1982), *Tracers in the sea*, 690 pp., Eldigio, New York.

Chase Z., R.F. Anderson, M.Q. Fleisher, and P.W. Kubik (2002), The influence of particle composition and particle flux on scavenging of Th, Pa and Be in the ocean, *Earth Planet. Sci. Lett.*, *204*, 215–229.

Chase Z., R.F. Anderson, M.Q. Fleisher, and P.W. Kubik (2003), Scavenging of ^{230}Th, ^{231}Pa and ^{10}Be in the Southern Ocean (SW Pacific Sector): The importance of particle flux, particle composition and advection, *Deep Sea Res. II*, *50*, 739–768.

Comiso, J.C. (2003), Large-scale characteristics and variability of the global sea ice cover, in *Sea Ice An Introduction to its Physics, Chemistry, Biology and Geology*, edited by D.N. Thomas and G.S. Diekmann, pp. 112-142, Blackwell, Oxford.

Conley, D.J. (1998), An interlaboratory comparison for the measurement of biogenic silica in sediments, *Mar. Chem.*, *63*, 39-48.

Cooke, D.W. and J. D. Hays (1982), Estimates of Antarctic Ocean seasonal sea-ice cover during glacial intervals, in *Antarctic Geoscience, Third Symposium on Antarctic Geology and Geophysics, Madison, Wisconsin, U.S.A., August 22-27, 1977*, edited by C. Craddock, International Union of Geological Sciences (IUGS), Oslo.

de Baar, H.J.W., J.T.M. de Jong, D.C.E. Bakker, B.M. Loescher, C.Veth, U.V. Bathmann, and V. Smetacek (1995), Importance of iron for plankton blooms and carbon dioxide drawdown in the southern ocean, *Nature*, *373*, 412-415.

DeMaster, D.J. (1979), The marine budgets of silica and ^{32}Si, Ph.D. Thesis, Yale University, 1979.

DeMaster, D.J. (1981), The supply and accumulation of silica in the marine environment, *Geochim. Cosmochim. Acta*, *45*, 1715-1732.

DeMaster, D.J., T.M. Nelson, S.L. Harden, and C.A. Nittrouer (1991), The cycling and accumulation of biogenic silica and organic carbon in Antarctic deep-sea and continental margin environments, *Mar. Chem.*, *35*, 489-502.

DeMaster, D.J. (2002), The accumulation and cycling of biogenic silica in the Southern Ocean: revisiting the marine silica budget, *Deep Sea Res. II*, *49 (16)*, 3155-3167.

Dezileau, L., G. Bareille, J.L. Reyss, and F. Lemoine (2000), Evidence for strong sediment redistribution by bottom currents along the southeast Indian ridge, *Deep Sea Res. I*, *47,* 1899-1936.

Dezileau, L., J.L. Reyss, and F. Lemoine (2003), Late Quaternary changes in biogenic opal fluxes in the Southern Indian Ocean, *Mar. Geol.*, *202 (3-4)*, 143-158.

François, R., M. Bacon, P. M. Altabet, and L. D. Labeyrie (1993), Glacial/Interglacial changes in sediment rain rate in the SW Indian sector of subantarctic waters as recorded by ^{230}Th, ^{231}Pa, U and ^{15}N, *Paleoceanography*, *8*, 611-629.

François, R., M.A. Altabet, E.-F. Yu, D. Sigman, M.P. Bacon, M. Frank, G. Bohrmann, G. Bareille, and L.D. Labeyrie (1997), Contribution of southern ocean surface water stratification to low atmospheric CO_2 concentrations during the last glacial period, *Nature 389*, 929-935.

François, R., M. Frank, M.M. Rutgers van der Loeff, and M.P. Bacon (2004), ^{230}Th normalization: An essential tool for interpreting sedimentary fluxes during the late Quaternary, *Paleoceanography*, *19*, PA1018, doi:10.1029/2003PA000939.

Frank, M. (1996), Reconstruction of Late Quaternary environmental conditions applying the natural radionuclides ^{230}Th, ^{231}Pa and ^{238}U: A study of deep-sea sediments from the eastern sector of the Antarctic Circumpolar Current System, *Reports on Polar Research*, *186*, 136 pp., Alfred Wegener Inst. for Polar and Marine Research, Bremerhaven.

Frank, M., R. Gersonde, and A. Mangini (1999), Sediment redistribution, $^{230}Th_{ex}$-normalization and implications for the reconstruction of particle flux and export paleoproductivity, in *Use of Proxies in Paleoceanography: Examples from the South Atlantic*, edited by G. Fischer and G. Wefer, Springer, Berlin, Heidelberg, New York, 409-426.

Frank, M., R. Gersonde, M. M. Rutgers van der Loeff, G. Bohrmann, C. C. Nürnberg, P.W. Kubik, M. Suter, and A. Mangini (2000), Similar glacial and interglacial export bioproductivity in the Atlantic sector of the Southern Ocean: multiproxy evidence and implications for glacial atmospheric CO_2, *Paleoceanography*, *15*, 642-658.

Geibert, W. and Usbeck, R. (2004), Adsorption of thorium and protactinium onto different particle types: experimental findings, *Geochim. Cosmochim. Acta*, *68 (7)*, 1489-1501.

Geibert, W., C. Hanfland, J. Schwarz, R. Usbeck, A. Webb, and I. Ansorge (2004), Ocean circulation and bioproductivity in the Weddell Gyre: geochemical findings, *Geochim. Cosmochim. Acta*, *68, 11S,* A331.

Henderson, G.M., C. Heinze, R.F. Anderson, and A.M.E. Winguth (1999), Global distribution of the ^{230}Th flux to the ocean sediments constrained by GCM modeling, *Deep Sea Res. I*, *46*, 1861-1893.

Leynaert, A., D. M. Nelson, B. Quéguiner and P. Tréguer (1993), The silica cycle in the Antarctic Ocean: is the Weddell Sea atypical?, *Mar. Ecol. Prog. Ser.*, *96*, 1-15.

Lisitzin, A. P. (1971), Distribution of siliceous microfossils in suspension and in bottom sediments, in *The Micropalaeontology of Oceans*, edited by B. M. Funnell and W. R. Riedel, pp. 173-195, Cambridge University Press, Cambridge, UK.

Lisitzin, A. P. (1985), The silica cycle during the last ice age, *Palaeogeography, Palaeoclimatology, Palaeoecology*, *50*, 241-270.

Lisitzin, A. P. (1996), *Oceanic Sedimentation*, AGU, Washington, D.C.

Mollenhauer, G., Schneider, R. R., Müller, P. J., Spieß, V., and Wefer, G. (2002), Glacial/interglacial variability in the Benguela upwelling system: Spatial distribution and budgets of organic carbon accumulation, *Global Bigeochem. Cycles*, *16 (4)*, 1134, doi:10.1029/2001GB001488.

Moore, J.K., M.R. Abbott, and J.G. Richman (1999), Location and dynamics of the Antarctic Polar Front from satellite sea surface temperature data, *J. Geophys. Res.*, *104 (C2)*, 3059-3073.

Müller, P. J. and R. Schneider (1993), An automated method for the determination of opal in sediments and particulate matter, *Deep Sea Res. I*, *40 (3)*, 425-444.

Nelson, D. M., P. Tréguer, M. A. Brzezinski, A. Leynaert, and B. Quéguiner (1995), Production and dissolution of biogenic silica in the ocean: Revised global estimates, comparison with regional data and relationship to biogenic sedimentation, *Global Biogeochem. Cycles*, *9*, 359-372.

Nelson, D.M. et al. (2002), Vertical budgets for organic carbon and biogenic silica in the Pacific sector of the Southern Ocean, 1996-1998, *Deep Sea Res. II*, *49 (9-10)*, 1645-1674.

Orsi, A. H., T. Whitworth and W. D. Nowlin (1995), On the meridional extent and fronts of the Antarctic Circumpolar Current, *Deep Sea Res. I*, *42*, 641-673.

Pondaven, P., O. Ragueneau, P. Tréguer, A. Hauvespre, L. Dezileau, and J. L. Reyss (2000), Resolving the 'opal paradox' in the Southern Ocean, *Nature*, *405*, 168-169.

Ragueneau, O. et al. (2000), A review of the Si cycle in the modern ocean: recent progress and missing gaps in the application of biogenic opal as a paleoproductivity proxy, *Global Planet. Change*, *26*, 317-365.

Rutgers van der Loeff, M. M. and G. W. Berger (1993), Scavenging of ^{230}Th and ^{231}Pa near the Antarctic Polar Front in the South Atlantic, *Deep Sea Res. I*, *40*, 339-357.

Sayles, F. L., W.R. Martin, Z. Chase, and R. F. Anderson (2001), Benthic remineralization and burial of biogenic SiO_2, $CaCO_3$, organic carbon, and detrital material in the Southern Ocean along a transect at 170° West, *Deep Sea Res. II, 48 (19-20)*, 4323-4383.

SeaWiFS, http://seawifs.gsfc.nasa.gov/SEAWIFS.html, 2004

Schlitzer, R., Ocean Data View, http://www.awi-bremerhaven.de/GEO/ODV, 2004.

Schlüter, M. and Rickert, D. (1998), Effect of pH on the measurement of biogenic silica, *Mar. Chem.*, *63*, 81-92.

Schlüter, M., M. M. Rutgers van der Loeff, O. Holby, and G. Kuhn (1998), Silica Cycle in Surface Sediments of the South Atlantic, *Deep Sea Res. II*, *45*, 1085-1109.

Suman, D. O. and M. P. Bacon (1989), Variations in Holocene sedimentation in the North American basin determined from ^{230}Th measurements, *Deep Sea Res., 36*, 869– 878.

Thomson, C.W. and J. Murray, (1891), *Report on the Scientific Results of the Voyage of H.M.S. Challenger during the Years 1873-76 Deep-Sea deposits*, 583 pp., Her Majesty´s Stationery Office, London, Edinburg, Dublin.

Thomson, J., S. Colley, R. Anderson, G.T. Cook, A.B. MacKenzie, and D.D. Harkness (1993), Holocene sediment fluxes in the Northeast Atlantic from $^{230}Th_{excess}$ and radiocarbon measurements, *Paleoceanography*, *8*, 631-650.

Tomczak, M. and J.S. Godfrey (1994), *Regional Oceanography: An Introduction*, 422 pp., Pergamon, Oxford.

Tréguer, P. and A.J. van Bennekom (1991), The annual production of biogenic silica in the Antarctic Ocean, *Mar. Chem.*, *35*, 477-487.

Tréguer, P., D.M. Nelson, A.J. Van Bennekom, D.J. DeMaster, A. Leynaert, and B. Quéguiner (1995), The silica balance in the world ocean: A re-estimate, *Science*, *268*, 375-379.

Usbeck, R. (1999), Modeling of marine biogeochemical cycles with an emphasis on vertical particle fluxes, *Reports on Polar Research*, *332*, 105 pp., Alfred Wegener Inst. for Polar and Marine Research, Bremerhaven.

Usbeck, R., M.M. Rutgers van der Loeff, M. Hoppema, and R. Schlitzer (2002), Shallow remineralization in the Weddell Gyre, *Geochem. Geophys. Geosyst.*, *3 (1)*, 10.1029/2001GC000182.

van Bennekom, A. J., G. W. Berger, S. J. van der Gaast, and R. T. P. de Vries (1988), Primary productivity and the silica cycle in the Southern Ocean (Atlantic sector), *Palaeogeography, Palaeoclimatology, Palaeoecology*, *67*, 19-30.

Walter, H.J., M.M. Rutgers van der Loeff, and H. Hoeltzen (1997), Enhanced scavenging of ^{231}Pa relative to ^{230}Th in the South Atlantic south of the Polar Front: Implications for the use of the ^{231}Pa/^{230}Th ratio as a paleoproductivity proxy, *Earth Planet. Sci. Lett.*, *149*, 85-100.

Walter, H.J., M.M. Rutgers van der Loeff, H. Hoeltzen, and U. Bathmann (2000), Reduced scavenging of ^{230}Th in the Weddell Sea: implications for paleoceanographic reconstructions in the South Atlantic, *Deep Sea Res. I*, *47*, 1369-1387.

Yu, E.-F., R. François, M. P.Bacon, and A.P. Fleer (2001), Fluxes of ^{230}Th and ^{231}Pa to the deep sea: Implications for the interpretation of excess ^{230}Th and ^{231}Pa/^{230}Th profiles in sediments, *Earth Planet. Sci. Lett*., *91*, 219– 230.

Zielinski, U. and R. Gersonde (1997), Diatom distribution in Southern Ocean surface sediments: Implications for paleoenvironmental reconstructions, *Palaeogeography, Palaeoclimatology, Palaeoecology*, *129*, 213-250, 1997.

Zielinski, U., R. Gersonde, R. Sieger, and D. Fütterer (1998), Quaternary surface water temperature estimations: Calibration of a diatom transfer function for the Southern Ocean, *Paleoceanography*, *13 (4)*, 365-383.

Figure captions

Figure 1: Weight percent biogenic opal (including 10% H_2O) in surface sediments of the South Atlantic and South Pacific. Please note the non-linear color scale. Frontal Features (according to Orsi et al. 1995) are shown in grey. From North to South: Subtropical Front (STF), Subantarctic Front (SAF), Antarctic Polar Front (APF), Southern ACC boundary. Dotted white line: Northern boundary of 15% sea-ice cover in August according to *Comiso* [2003]. Dashed black line: Boundary of siliceous ooze deposits according to *DeMaster* [2002].

Figure 2: $^{230}Th_{ex}$ [dpm*g^{-1}, dry sediment] in the study area. Please note the non-linear color scale, which was chosen to allow better discrimination of low Thorium contents.

Figure 3: Thorium-normalized preserved vertical sediment fluxes ($^{pr}F_v^{tot}$) in g*m^{-2}*yr^{-1} (calculation see section 2.4)

Figure 4: ^{230}Th-corrected preserved vertical silica fluxes ($^{pr}F_v^{Si}$) (in mmol*m^{-2}*yr^{-1}) with consideration of Th-advection in the Weddell Gyre according to *Walter et al.* [2000].

Figure 5 The definition of regions for the calculation of spatial budgets in the area of investigation. The coloured dots give the preserved vertical silica flux in mmol*m^{-2}*yr^{-1}. Dotted lines represent the boundaries of the respective regions. Numbers in circles designate the numbers of the regions. 1: PFZ+SAZ, Atlantic sector; 2: POOZ, Atlantic sector; 3: Western Weddell Gyre; 4: Eastern Weddell Gyre; 5: PFZ+SAZ, Indian sector; 6: POOZ, Indian sector; 7: POOZ, Pacific Sector; 8: POOZ, Southeast Pacific sector; 9: PFZ+SAZ, Southeast Pacific sector.

Tables

Table 1: Total vertical fluxes to the sediment ($^{pr}F_v^{tot}$), biogenic opal contents, mean vertical silica fluxes ($^{pr}F_v^{Si}$) and regional silica fluxes to several provinces of the Southern Ocean. Provinces defined as designated in Figure 5. The error means the respective standard deviation; further explanations are given in the text.

Ocean basin	**Province**	**Surface Area [cm²]**	**$^{pr}F_v^{tot}$ [g/m²/y] ± 1 SD**	**n**	**biogenic opal content [%] ± 1 SD**	**n**	**$^{pr}F_v^{Si}$ [mmol/m²/y] ± 1 SD**	**n**	**Si flux [mol/yr] ± 1 SD**
Atlantic Ocean	PFZ+SAZ	$7.4*10^{16}$	10.9 ± 7.0	17	13.8 ± 8.7	18	16 ± 6	16	$1.2*10^{11} \pm 0.5*10^{11}$
Atlantic Ocean	POOZ	$4.6*10^{16}$	13.9 ± 5.7	33	31.1 ± 14.4	40	61 ± 29	31	$2.8*10^{11} \pm 1.3*10^{11}$
Atlantic Ocean	Western Weddell Gyre	$2.5*10^{16}$	4.1 ± 1.3	21	1.9 ± 1.6	55	0.7 ± 0.1	15	$1.7*10^{9} \pm 0.3*10^{9}$
Atlantic Ocean	Eastern Weddell Gyre	$3.1*10^{16}$	2.9 ± 0.9	13	10.6 ± 7.6	49	6.3 ± 3.2	7	$2.0*10^{10} \pm 1.0*10^{10}$
Atlantic Ocean	**Entire South Atlantic**	**$1.8*10^{17}$**	-	**84**	-	**162**	-	**69**	**$4.2*10^{11} \pm 1.4*10^{11}$**
Indian Ocean	PFZ+SAZ	-	-	2	-	2	-	2	-
Indian Ocean	POOZ	-	15.8 ± 9.3	5	42.4 ± 9.6	6	103 ± 60.3	5	-
South Pacific	POOZ	-	6.2 ± 2.3	8	61.8 ± 24.3	8	50 ± 21	8	-
Southeast Pacific	POOZ	$2.2*10^{16}$	5.9 ± 2.3	16	12.1 ± 5.1	16	10.2 ± 4.5	16	$2.2*10^{10} \pm 1.0*10^{10}$
Southeast Pacific	PFZ+SAZ	$2.9*10^{16}$	3.0 ± 2.3	12	18.2 ± 9.0	12	6.2 ± 2.6	12	$1.8*10^{10} \pm 0.7*10^{10}$
Southeast Pacific	**Entire Southeast Pacific**	**$5.1*10^{16}$**	-	**28**	-	**28**	-	**28**	**$4.0*10^{10} \pm 1.2*10^{10}$**

Table 2: A compilation of the currently available best estimates of vertical silica fluxes (Th-normalized) into the sediment in the Southern Ocean. Values are given in mmol*m^{-2}*yr^{-1}.

Region (reference)	**PFZ**[1]		**POOZ**		**SIZ**	
Atlantic (this work)	16 ± 6	n=16	61 ± 29	n=31	Weddell Gyre	-
Eastern Weddell Gyre (this work)	-	-	-	-	6.3 ± 3.2	n=7
Western Weddell Gyre (this work)	-	-	-	-	0.7 ± 0.1	n=15
Pacific 90°W (this work)	6.2 ± 2.6	n=12	10.2 ± 4.5	n=16	like POOZ	-
Pacific 115° W (this work)	no data	-	50 ± 21	n=8	not sufficient data	-
Pacific 170° W [*Sayles et al*., 2001]	9-48	n=4	89-273	n=3	not sufficient data	-
Indian Ocean 62°E [*Pondaven et al.*, 2000]	75 ± 42	n=?	210 ± 40	n=?	not sufficient data	-
Indian Ocean 73-110 °E [*Dezileau et al.*, 2003]	10-35	n=4	216 and 297	n=2	not sufficient data	-

[1]values for the PFZ from this work additionally include the SAZ

Figures

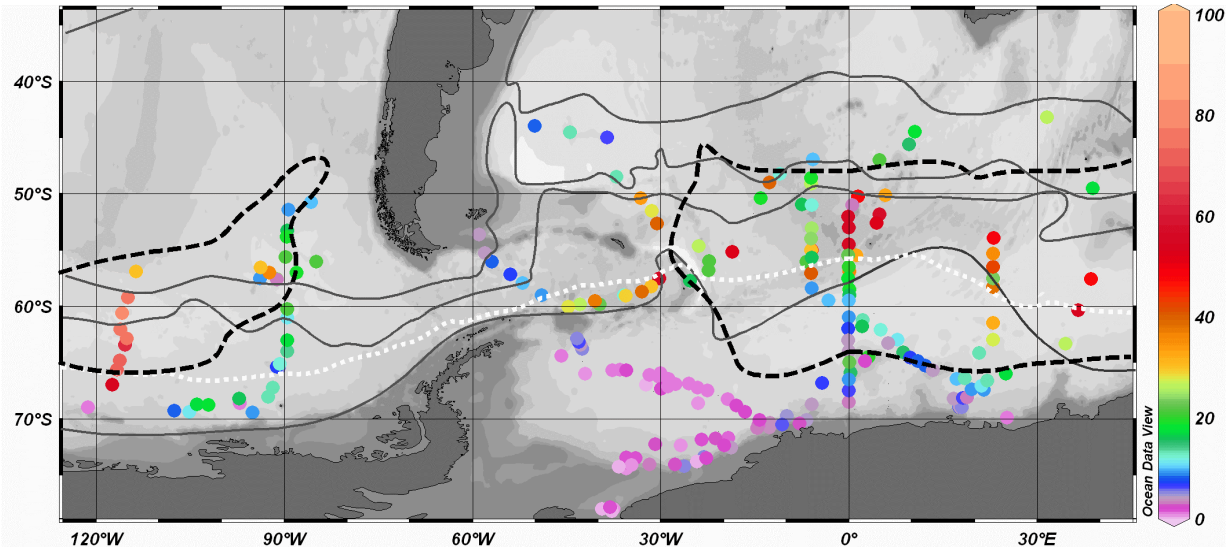

Figure 1

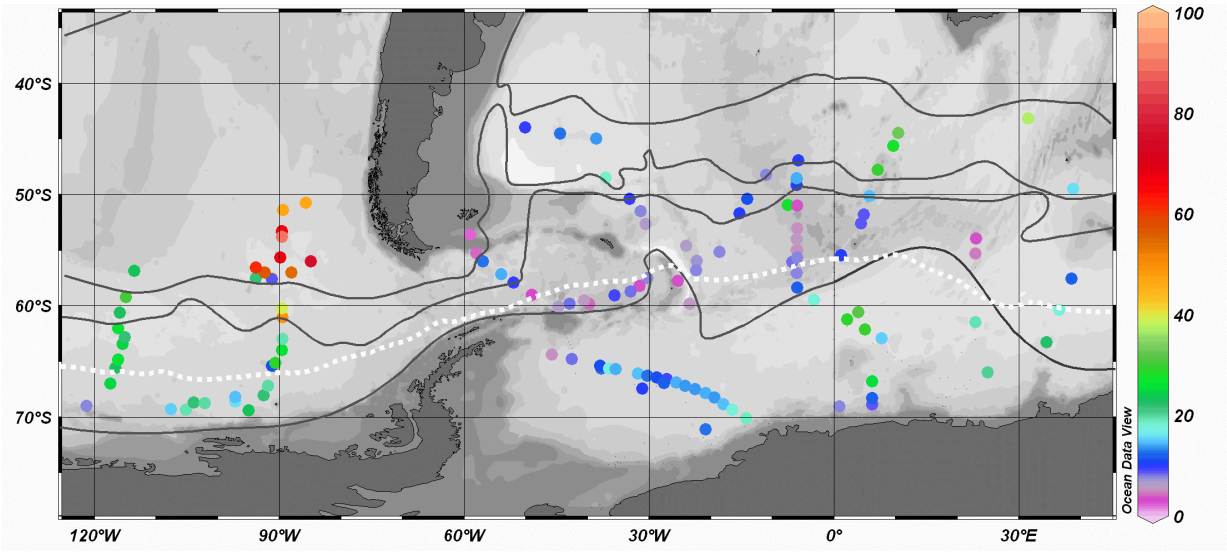

Figure 2

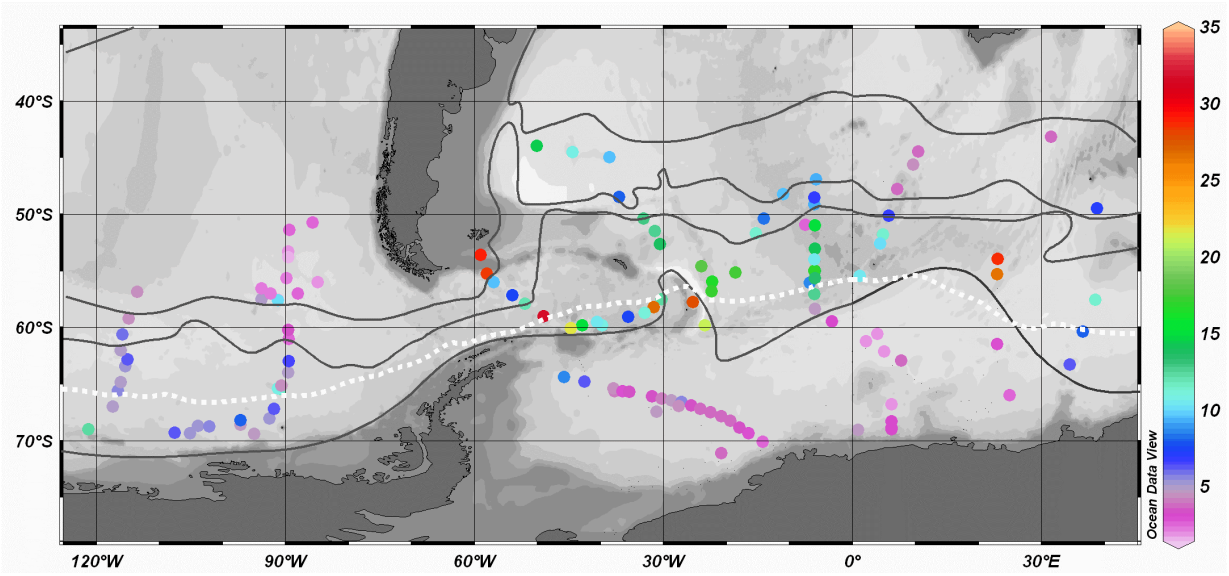

Figure 3

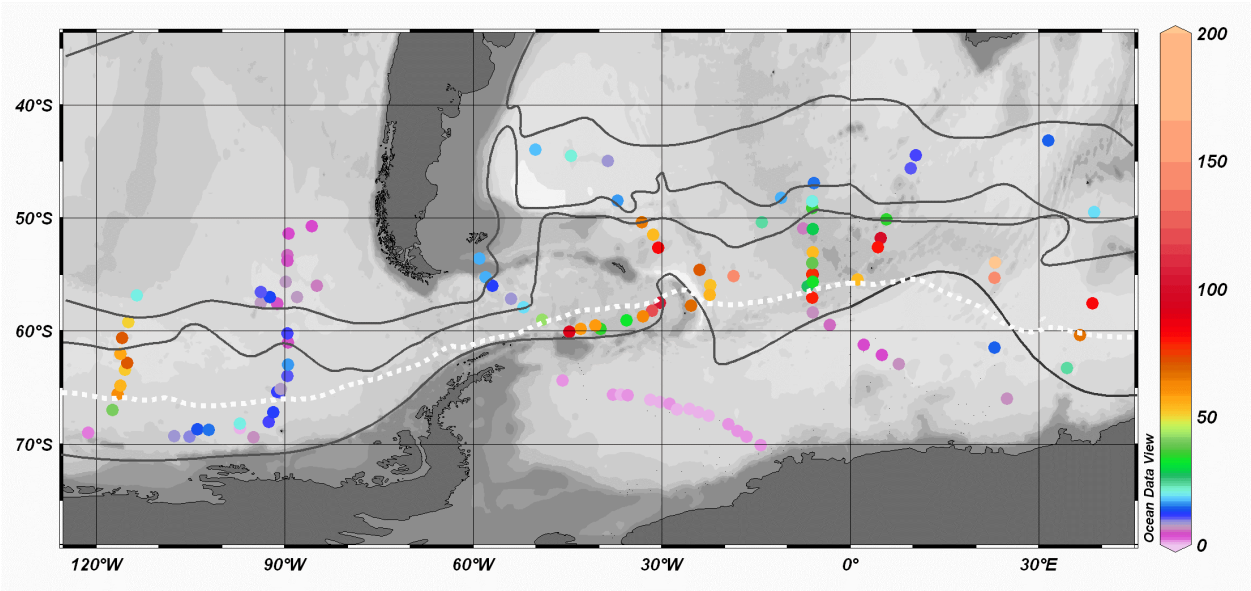

Figure 4

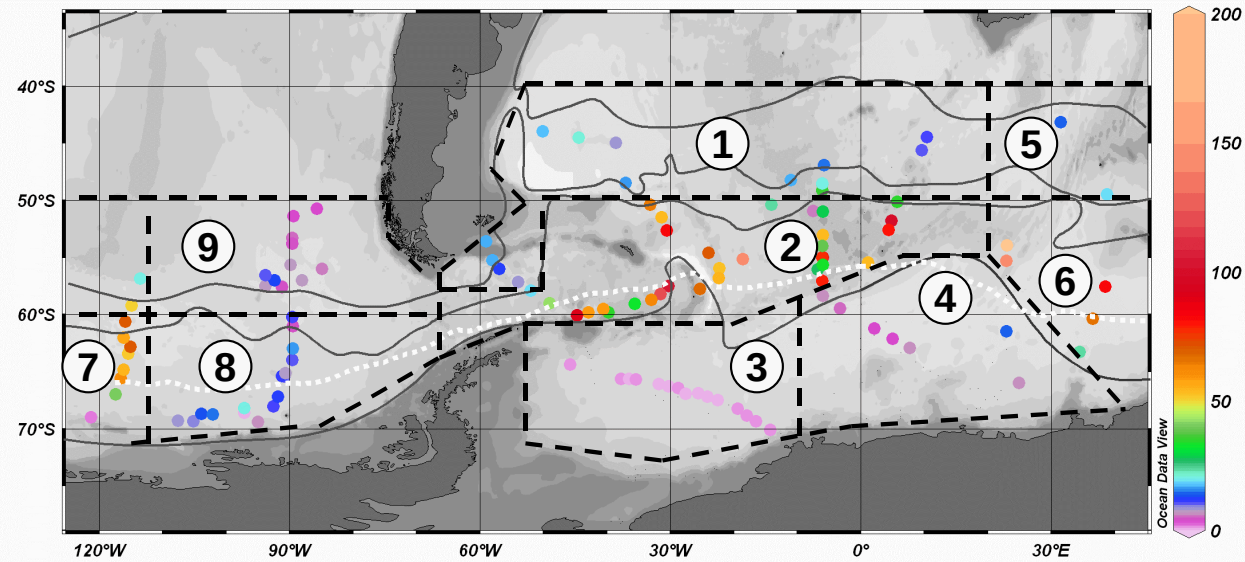
40°S
50°S
60°S
70°S
120°W
90°W
60°W
30°W
0°
30°E
1
2
3
4
5
6
7
8
9
200
150
100
50
0
Ocean Data View

Figure 5